Regulated spindle orientation buffers tissue growth in the epidermis

Angel Morrow[1,3], Julie Underwood[3], Lindsey Seldin[2], Taylor Hinnant and Terry Lechler

Departments of Dermatology and Cell Biology, Duke University, Durham NC 27710
[1]present address – Novozymes, Durham, NC
[2]present address Department of Cell and Developmental Biology, Vanderbilt University, Nashville TN
[3]Equal contributions

Corresponding Author:
Terry Lechler
Depts. of Dermatology and Cell Biology
Duke University Medical Center
310 Nanaline Duke Bldg, Box 3709
Durham, NC 27710
USA
Phone: 919 684-4550
Fax: 919 684-5481
Email: terry.lechler@duke.edu

Summary

Tissue homeostasis requires a balance between progenitor cell proliferation and loss. Mechanisms that maintain this robust balance are needed to avoid tissue loss or overgrowth. Here we demonstrate that regulation of spindle orientation/asymmetric cell divisions is one mechanism that is used to buffer changes in proliferation and tissue turnover in mammalian skin. Genetic and pharmacologic experiments demonstrate that asymmetric cell divisions were increased in hyperproliferative conditions and decreased under hypoproliferative conditions. Further, active K-Ras also increased the frequency of asymmetric cell divisions. Disruption of spindle orientation in combination with constitutively active K-Ras resulted in massive tissue overgrowth. Together, these data highlight the essential roles of spindle orientation in buffering tissue homeostasis in response to perturbations.

Results

The epidermis is a proliferative tissue that turns over repeatedly throughout life. Remarkably, in aged sun-exposed skin, homeostasis and the architecture of the epidermis is maintained despite prevalent clones of cells containing oncogenic mutations [1]. Recent work has highlighted oncogene-induced differentiation and active elimination of mutant clones as two mechanisms of epidermal robustness, suggesting there are multiple modes of response to perturbation [2, 3]. Homeostasis requires that gain of cells (proliferation) must be balanced with loss of cells (differentiation or cell death). One possible mechanism to control homeostasis is regulated spindle orientation and asymmetric cell divisions. These divisions do not increase progenitor number, but rather commit one daughter to differentitiation. Embryonic epidermal progenitors can divide parallel to the basement membrane, resulting in two basal daughter cells, which we term symmetric divisions. These cells can also divide perpendicular to the basement membrane [4-7]. Perpendicular divisions are termed asymmetric divisions because they contribute one daughter cell to the differentiated suprabasal cell layer and do not alter the number of basal progenitor cells. Because of these properties, regulated spindle orientation is a candidate for providing resilience to homeostatic perturbation. In the embryonic epidermis, asymmetric divisions are used to drive stratification of the skin [4, 6, 7]. However, in adult backskin most divisions are planar (symmetric) and the utility of regulated spindle orientation has not been explored [8, 9]. Here, we examine the possibility that regulated spindle orientation can buffer the effects of perturbed homeostasis.

To begin to test this idea, we first examined whether spindle orientation was altered when developmental or adult homeostatic proliferation was experimentally altered. In the embryonic mouse epidermis, where proliferation is high, the ratio of perpendicular to planar divisions is approximately 70:30 [4, 6]. To inhibit basal cell cycle progression, we used a basal epidermal keratin 14 promoter to drive a doxycycline-inducible allele of Cdkn1b, a CDK1 inhibitor (K14-rtTA;tetO-CDKN1b) [10]. Quantitation of the percentage of cells expressing the mitotic marker phospho-histone H3 (pHH3) revealed a significant decrease in basal cell proliferation (Fig. 1A). This also resulted in a significant reduction in perpendicular divisions, from 70% to 35%, with a concomitant increase in planar divisions (from 22% to 42%) (Fig. 1B,C). This is consistent with the need for increased rates of planar divisions to maintain the surface area of the epidermis in a rapidly growing embryo.

In contrast to the embryo, the proliferation rate in the adult backskin is low. Live imaging has shown that most divisions occur symmetrically and that basal cells delaminate from the basement membrane to populate suprabasal cell layers [8, 9]. Consistent with this observation, we see that the majority of mitotic spindles are planar in adult backskin (Fig. 1E). Notably, there is regional variability in epidermis from different anatomical areas in both proliferation and spindle orientation. The epidermis of the footpad, which is thicker, has both a higher proliferation index and increased numbers of perpendicular divisions (Supplemental Figure 1).

To induce hyperproliferation of adult backskin epidermis we topically applied the mitogen TPA. This resulted in thickening of the epidermis and a 6-fold increase in

proliferation rate as measured by BrdU incorporation (Fig. 1D). Notably, this treatment increased the percentage of perpendicular divisions from 20 to 40% (Fig. 1E,F). Therefore, one of the responses to TPA-induced hyperproliferation in the epidermis is an increase in the rate of divisions that give rise to differentiated progeny. Together these data demonstrate correlations between proliferation and spindle orientation, and support the hypothesis that cells tune their division orientation in response to the needs of the surrounding tissue as a mechanism to promote robust homeostasis.

To directly determine whether regulated spindle orientation was important for epidermal homeostasis we examined the effects of mutating the nuclear mitotic apparatus protein, NuMA, which is essential for spindle orientation in embryonic skin [7, 11]. We did not see significant phenotypes when we disrupted NuMA's spindle orientation function in adult epidermis for short times (data not shown), consistent with findings that adult backskin homeostasis is normally maintained by delamination and differentiation rather than by regulated spindle orientation [9].

Given that tissues responded to TPA-induced hyperproliferation by increasing perpendicular divisions, we next asked whether this also occurred in response to an oncogenic perturbation. Mutations that activate Ras family members can drive squamous cell carcinoma and a significant percentage of squamous tumors carry Ras mutations [12-14]. Unexpectedly, we found that expression of $KRAS^{G12D}$ (at endogenous levels and only in the epidermis; K5CreER;$KRAS^{G12D/+}$) had distinct effects in backskin and footpad epidermis. While there was no significant change in division orientation ratios in the backskin, active K-Ras resulted in an increase in perpendicular divisions in the

footpads (Fig. 2A-D). These data rule out the possibility that active K-Ras inhibits regulated spindle orientation/asymmetric cell divisions as an oncogenic mechanism. It raised the alternative possibility that the increased perpendicular divisions may protect the tissue against overgrowth. We therefore addressed the molecular requirements for spindle orientation in skin expressing active K-Ras. We combined a NuMA mutation that disrupts embryonic spindle orientation with the $KRAS^{G12D}$ oncogene [11, 15]. This resulted in a significant shift of divisions from perpendicular to planar, consistent with NuMA being required for spindle orientation in this context (Fig. 2E).

The consequence of perturbing regulated spindle orientation in epidermis expressing active KRAS was dramatic. Within two weeks of recombination, large overgrowths appeared on the footpads and anogenital regions of the double mutant mice ($K5Cre^{ER}$;$KRAS^{G12D/+}$;$NuMA^{MTBDfl/fl}$)(Fig. 3A). These features were not found in single $KRAS^{G12D}$ or NuMA mutants, although $KRAS^{G12D}$ alone was sufficient for formation of oral tumors similar to those that appeared in the double mutants. Most mice died within 3-4 weeks after recombination (Fig. 3B).

Histologic analysis of the double mutant paws demonstrated massive tissue overgrowth and papilloma formation (Fig. 3D-G). Despite this dramatic change in tissue architecture, the basement membrane remained intact and differentiation was normal at early time points. Thus, this combination of mutations is not sufficient for invasion, at least in the short time period we were able to assay. The massive tissue overgrowth led to lethality, likely due, at least in part, to blockage of the oral cavity.

Similar to the loss of NuMA function in the adult epidermis, loss of spindle orientation alone is not detrimental in developing fly wings [16]. However, tumors forms when combined with additional mutations that inhibited apoptosis. Notably, we saw no genetic interaction when mutant p53 was combined with the NuMA$^{\Delta MTBD}$ deletion (Fig. 3C). These data are consistent with the fact that apoptosis is not a major determinant of tissue homeostasis in the epidermis under normal conditions, and demonstrates a specificity for disrupted spindle organization working synergistically with only a subset of oncogenic drivers.

Histologic analysis revealed expansion of the stem cell pool in the KRAS^{G12D}; NuMA$^{\Delta MTBD}$ epidermis. To accommodate the increase in cell numbers, the basement membrane became highly involuted (Fig. 3D-G). We quantitated this as basement membrane length per tissue length and found a 2-4 fold increase in this measure, corresponding to a 4-16 fold increase in area (Fig. 3H). As cell density was not notably altered, this demonstrates an expansion of the basal stem cell pool. These data are consistent with regulated spindle orientation buffering the effects of oncogenic K-Ras. Similarly, we found that low-dose TPA treatment caused a subtle yet significant increase in basement membrane length in NuMA$^{\Delta MTBD}$ mice as compared to control mice (Supplemental Figure 2).

Active K-Ras has both proliferative and anti-differentiative effects in different tissues. Because increased proliferation can drive increased asymmetric divisions (Fig. 1), we asked whether the changes observed in K-Ras mutant skin could be due to

oncogene-induced hyperproliferation. Notably, we found that constitutively active KRas expression is not sufficient to drive hyperproliferation in the paw skin (Fig. 3I).

Previous work has suggested that active Ras can inhibit differentiation when overexpressed in the epidermis [17]. However, this has not been examined either in the adult pawskin or under endogenous levels of expression. In adults, cells commit to differentiation, detach from the basement membrane, and move upward. A small proportion of basal cells express the differentiation marker keratin 10 (K10) and can be fluorescently labeled in mice using established mouse lines (K10-rtTA;TRE-H2B-GFP) [18](Fig. 3J). Consistent with these cells entering differentiation, they did not incorporate BrdU (43$\pm$2.4% for $K10^{-ve}$ basal cells verses 4$\pm$2.0% for $K10^{+ve}$ basal cells, n=3 mice). We quantitated differentiation by analyzing the percentage of basal cells that express keratin 10. Using the K10-rtTA;TRE-H2B-GFP genetic labeling system we found that differentiation was suppressed in $KRAS^{G12D}$ expressing cells (Fig. 3K). This was most dramatic in the paw epidermis, but was also observed in backskin to a lesser extent. While the mechanism underlying this suppression is not clear, we also found that the relative intensity of β4-integrin was increased in the mutant pawskin, in a similar manner to what was observed when K-Ras was overexpressed in the embryo [17] (Fig. 3L). Robust adhesion and signaling through integrins is known to promote progenitor cell fate, and thus may contribute to the changes in differentiation that we observed.

Together, our data demonstrate that the epidermis can respond to changes in homeostasis by altering mitotic spindle orientation. Increasing perpendicular (asymmetric) divisions in response to either increased proliferation or decreased

differentiation allows homeostasis to be reset without dramatically affecting tissue architecture. Our genetic analysis clearly shows that this is essential to prevent tissue overgrowth in an oncogenic background. In addition, we found that the epidermis responded differently to the same oncogenic insult at different anatomic sites. This likely reflects the differences in proliferation, differentiation, and rates of asymmetric cell division rates in different regions of the epidermis and suggests that distinct "second hits" may be needed to collaborate with oncogenes in tissues with different mechanisms of achieving homeostasis.

Our data are consistent with the idea that both regulated spindle orientation and delamination/differentiation can be used to buffer basal cell number. Disruption of either one was insufficient to induce homeostatic defects due to compensation by the other. However, blockade of both homeostatic buffers resulted in tissue overgrowth and progenitor cell expansion. Notably, squamous cell carcinomas have been reported to have increased rates of perpendicular divisions as compared to normal epidermis [19, 20]. It will be important to see whether regulated spindle orientation is protective against tumor development in these contexts.

MATERIALS AND METHODS

Mouse strains and tissue preparation

All animal work was approved by Duke University's Institutional Animal Care and Use Committee. Mouse strains used in this study were: K5Cre^{ER} (Gift from Brigid Hogan), NuMA-ΔMTBD [11, 15], KRAS^{G12D} [21], and p53$^{fl/fl}$ [22]. Mice were genotyped by PCR,

and both males and females were used for experiments from postnatal day 30 – 60. For BrdU incorporation experiments, mice were injected with 10 mg/kg BrdU (Sigma-Aldrich) and left for 75 mins prior to sacrifice. Paws and backskin were embedded in Optimal Cutting Temperature prior to freezing, and samples were stored at -80˚C. A cryostat was used to cut 10-µm thick sections.

Immunofluorescence

For immunofluorescent staining, 10-uM thick sections were fixed for 8 min in 4% PFA in PBS-T (containing 0.2% Triton X-100) or 3 min in -20C methanol. Samples were washed for 5 min in PBS-T, and then incubated in blocking buffer (5% normal goat serum, 5% normal donkey serum, and 3% bovine serum albumen in PBS-T) for 15 min. Sections were then incubated with primary antibody overnight at 4C (for anti-K5/K14), or for 15 min at room temperature (all other antibodies). After washing with PBS-T, sections were incubated with secondary antibody for 10 min at room temperature. Sections were washed again and then mounted in 90% glycerol in PBS with 2.5 mg/mL p-Phenylenediamine (Sigma-Aldrich). Antibodies used were: rat anti-β4-integrin (BD Biosciences), rabbit anti-pHH3 (Cell Signaling Technology), rat anti-BrdU and rabbit anti-NuMA (Abcam), chicken anti-Keratin5/Keratin14 (Lechler lab), rabbit anti-Keratin 10 (Covance). Images were collected using a Zeiss Azio Imager Z1 fluorescence microscope with Apotome attachment. Adobe Photoshop and ImageJ software were used to process images.

Hematoxylin and Eosin Staining

Tissue sections were fixed for 10 min in 10% PFA in distilled water. Slides were then submerged in Mayer's Hemotoxylin (Sigma-Aldrich) for 10 min, and then allowed to rinse in water for approximately 10 min. Slides were dipped 5-10 times in 10% Eosin in ethanol, then washed by dipping 10 times in 50% ethanol, 10 times in 70% ethanol, incubated 30 sec in 95% ethanol, and 1 min in 100% ethanol. Slides were then dipped in xylene, allowed to air dry, and mounted in Permount (Sigma-Aldrich).

Acknowledgements

We thank Don Cleveland, Elaine Fuchs and Steve Pruitt for mouse strains used in this study and members of the Lechler Lab for comments on the manuscript. This work was supported by grants R01-AR067203 and R01-AR055926 from NIAMS/NIH.

References

1. Martincorena, I., Roshan, A., Gerstung, M., Ellis, P., Van Loo, P., McLaren, S., Wedge, D.C., Fullam, A., Alexandrov, L.B., Tubio, J.M., et al. (2015). Tumor evolution. High burden and pervasive positive selection of somatic mutations in normal human skin. Science (New York, N.Y *348*, 880-886.
2. Brown, S., Pineda, C.M., Xin, T., Boucher, J., Suozzi, K.C., Park, S., Matte-Martone, C., Gonzalez, D.G., Rytlewski, J., Beronja, S., et al. (2017). Correction of aberrant growth preserves tissue homeostasis. Nature *548*, 334-337.
3. Ying, Z., Sandoval, M., and Beronja, S. (2018). Oncogenic activation of PI3K induces progenitor cell differentiation to suppress epidermal growth. Nature cell biology *20*, 1256-1266.
4. Lechler, T., and Fuchs, E. (2005). Asymmetric cell divisions promote stratification and differentiation of mammalian skin. Nature *437*, 275-280.
5. Poulson, N.D., and Lechler, T. (2010). Robust control of mitotic spindle orientation in the developing epidermis. The Journal of cell biology *191*, 915-922.
6. Smart, I.H. (1970). Variation in the plane of cell cleavage during the process of stratification in the mouse epidermis. The British journal of dermatology *82*, 276-282.
7. Williams, S.E., Beronja, S., Pasolli, H.A., and Fuchs, E. (2011). Asymmetric cell divisions promote Notch-dependent epidermal differentiation. Nature *470*, 353-358.
8. Ipponjima, S., Hibi, T., and Nemoto, T. (2016). Three-Dimensional Analysis of Cell Division Orientation in Epidermal Basal Layer Using Intravital Two-Photon Microscopy. PLoS One *11*, e0163199.
9. Rompolas, P., Mesa, K.R., Kawaguchi, K., Park, S., Gonzalez, D., Brown, S., Boucher, J., Klein, A.M., and Greco, V. (2016). Spatiotemporal coordination of stem cell commitment during epidermal homeostasis. Science (New York, N.Y *352*, 1471-1474.
10. Pruitt, S.C., Freeland, A., Rusiniak, M.E., Kunnev, D., and Cady, G.K. (2013). Cdkn1b overexpression in adult mice alters the balance between genome and tissue ageing. Nat Commun *4*, 2626.
11. Seldin, L., Muroyama, A., and Lechler, T. (2016). NuMA-microtubule interactions are critical for spindle orientation and the morphogenesis of diverse epidermal structures. Elife *5*.
12. Daya-Grosjean, L., Robert, C., Drougard, C., Suarez, H., and Sarasin, A. (1993). High mutation frequency in ras genes of skin tumors isolated from DNA repair deficient xeroderma pigmentosum patients. Cancer research *53*, 1625-1629.
13. Pierceall, W.E., Goldberg, L.H., Tainsky, M.A., Mukhopadhyay, T., and Ananthaswamy, H.N. (1991). Ras gene mutation and amplification in human nonmelanoma skin cancers. Mol Carcinog *4*, 196-202.
14. South, A.P., Purdie, K.J., Watt, S.A., Haldenby, S., den Breems, N.Y., Dimon, M., Arron, S.T., Kluk, M.J., Aster, J.C., McHugh, A., et al. (2014). NOTCH1 Mutations

Occur Early during Cutaneous Squamous Cell Carcinogenesis. The Journal of investigative dermatology *134*, 2630-2638.

15. Silk, A.D., Holland, A.J., and Cleveland, D.W. (2009). Requirements for NuMA in maintenance and establishment of mammalian spindle poles. The Journal of cell biology *184*, 677-690.
16. Nakajima, Y., Meyer, E.J., Kroesen, A., McKinney, S.A., and Gibson, M.C. (2013). Epithelial junctions maintain tissue architecture by directing planar spindle orientation. Nature *500*, 359-362.
17. Dajee, M., Tarutani, M., Deng, H., Cai, T., and Khavari, P.A. (2002). Epidermal Ras blockade demonstrates spatially localized Ras promotion of proliferation and inhibition of differentiation. Oncogene *21*, 1527-1538.
18. Muroyama, A., and Lechler, T. (2017). A transgenic toolkit for visualizing and perturbing microtubules reveals unexpected functions in the epidermis. Elife *6*.
19. Beck, B., Driessens, G., Goossens, S., Youssef, K.K., Kuchnio, A., Caauwe, A., Sotiropoulou, P.A., Loges, S., Lapouge, G., Candi, A., et al. (2011). A vascular niche and a VEGF-Nrp1 loop regulate the initiation and stemness of skin tumours. Nature *478*, 399-403.
20. Siegle, J.M., Basin, A., Sastre-Perona, A., Yonekubo, Y., Brown, J., Sennett, R., Rendl, M., Tsirigos, A., Carucci, J.A., and Schober, M. (2014). SOX2 is a cancer-specific regulator of tumour initiating potential in cutaneous squamous cell carcinoma. Nat Commun *5*, 4511.
21. Jackson, E.L., Willis, N., Mercer, K., Bronson, R.T., Crowley, D., Montoya, R., Jacks, T., and Tuveson, D.A. (2001). Analysis of lung tumor initiation and progression using conditional expression of oncogenic K-ras. Genes & development *15*, 3243-3248.
22. Marino, S., Vooijs, M., van Der Gulden, H., Jonkers, J., and Berns, A. (2000). Induction of medulloblastomas in p53-null mutant mice by somatic inactivation of Rb in the external granular layer cells of the cerebellum. Genes & development *14*, 994-1004.

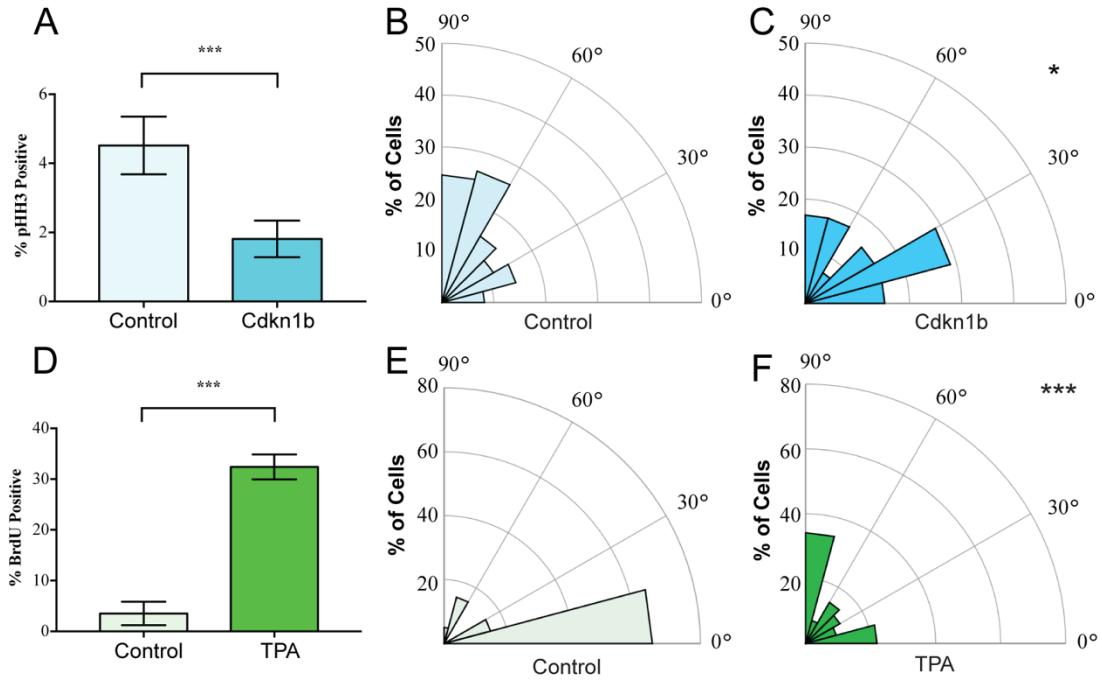

Figure 1: Mitotic spindles reorient in response to changes in proliferation. (A) Proliferation of control and K14-rtTA;TRE-Cdkn1b embryonic epidermis measured by pHH3 incorporation after treatment with doxycycline from e14.5-16.5. (B-C) Radial histograms of mitotic spindle orientation for e16.5 control (n = 61) and Cdkn1b (n = 59) embryonic epidermis. (D) Proliferation of adult backskin epidermis, control or TPA-treated (details), as measured by BrdU incorporation. (E-F) Radial histograms of mitotic spindle orientation for control (n = 20) and TPA-treated (n = 41) epidermis.

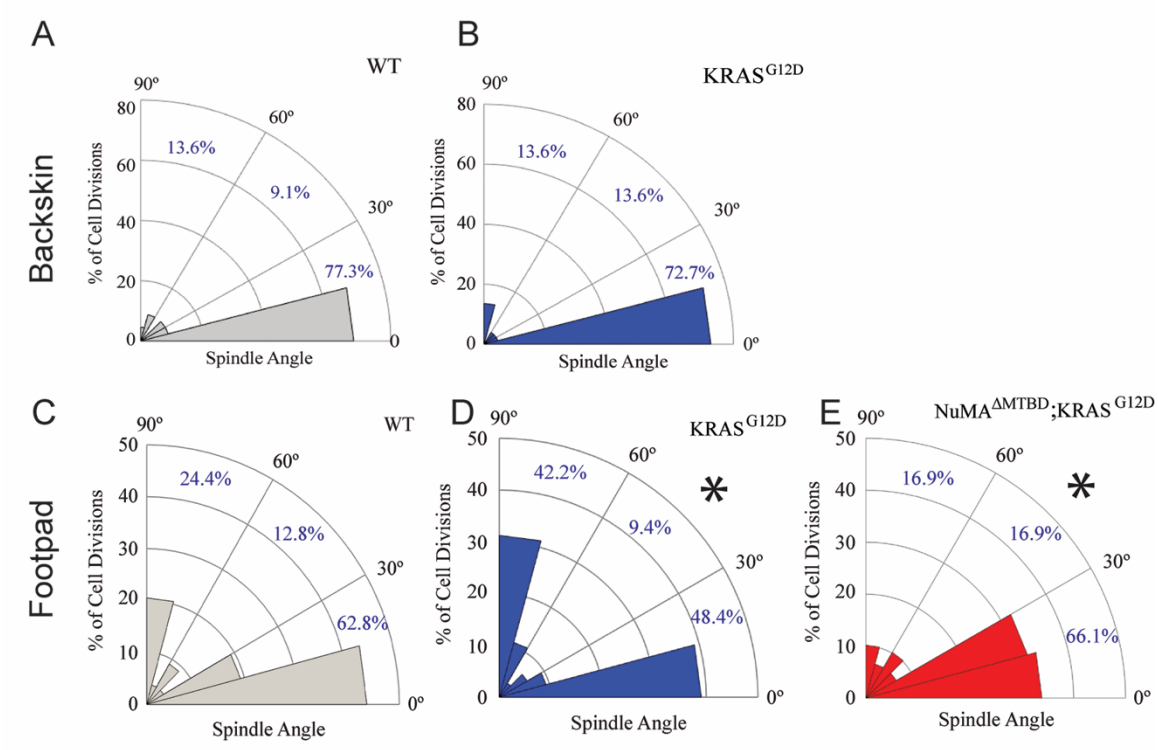

Figure 2: Oncogenic KRAS alters footpad epidermis spindle orientation in a NuMA-dependent manner. (A,B) Radial histogram of mitotic spindles in adult backskin 21 days after tamoxifen-induced recombination in control (A) and *K5Cre^{ER}; KRAS^{G12D}* mice (B). (C,D) Radial histogram of mitotic spindles in adult footpad epidermis, 21 days after tamoxifen-induced recombination in control (C) and *K5Cre^{ER}; KRAS^{G12D}* mice (D) (n=64 cells). (E) Radial histogram of mitotic spindles in adult footpad 21 days after tamoxifen-induced recombination in *K5Cre^{ER}; KRAS^{G12D};NuMA$^{\Delta MTBD}$* mice.

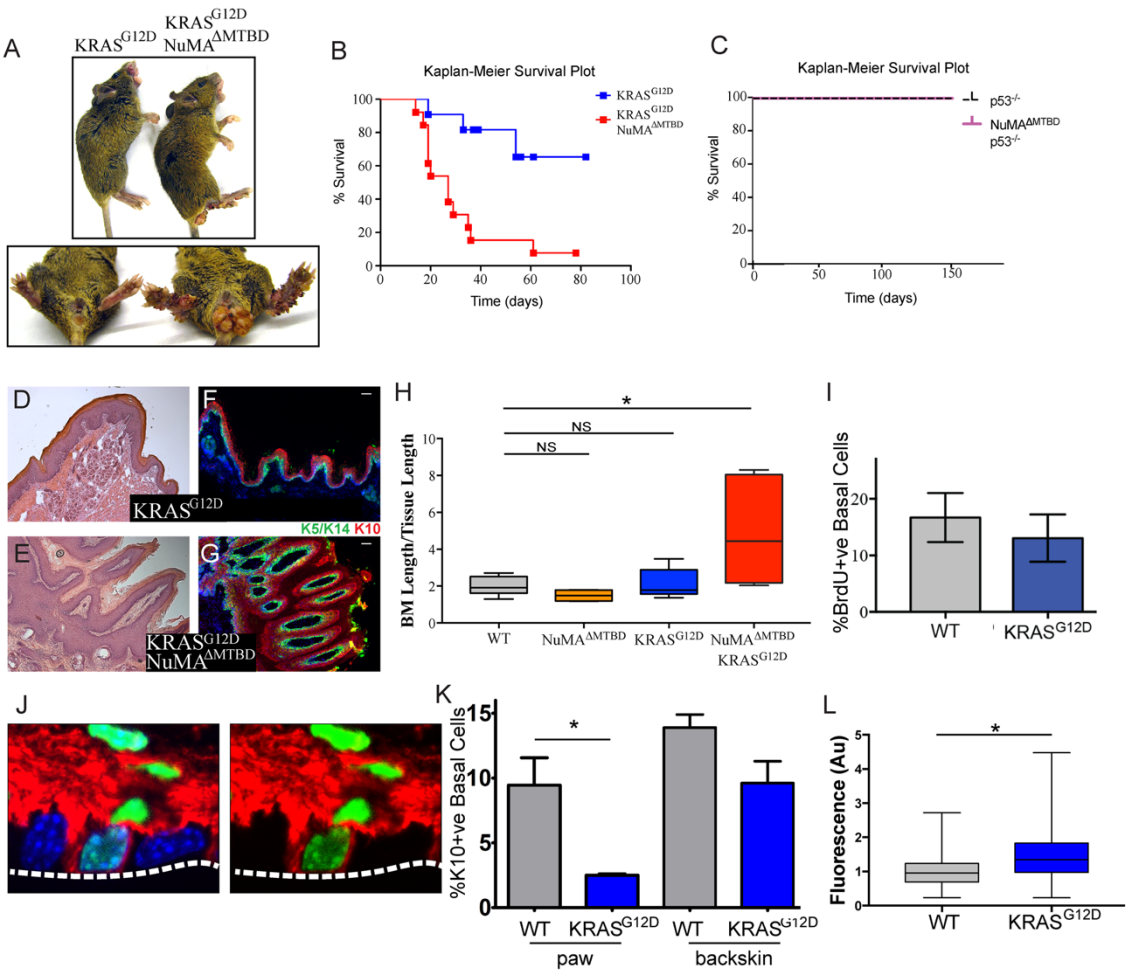

Figure 3: Loss of regulated spindle orientation synergizes with oncogenic KRAS to cause tissue overgrowth. (A) Images of *K5Cre^{ER}; KRAS^{G12D}* and *K5Cre^{ER}; NuMA$^{\Delta MTBD}$; KRAS^{G12D}* mice 21 days after recombination with tamoxifen, with inset of footpad and anal-genital region. (B,C)) Kaplan-Meier Survival plot of *K5Cre^{ER}; KRAS^{G12D}* and *K5Cre^{ER}; NuMA$^{\Delta MTBD}$; KRAS^{G12D}* mice (B) and *K5Cre^{ER}; p53$^{-/-}$* and *K5Cre^{ER}; p53$^{-/-}$; NuMA$^{\Delta MTBD}$* mice (C). (D,E) H&E images of *K5Cre^{ER}; KRAS^{G12D}* (D) and *K5Cre^{ER}; NuMA$^{\Delta MTBD}$; KRAS^{G12D}* (E) footpad epidermis. (F,G) Immunofluorescence images of *K5Cre^{ER}; KRAS^{G12D}* (F) and *K5Cre^{ER}; NuMA$^{\Delta MTBD}$; KRAS^{G12D}* (G) footpad epidermis showing localization of K5/K14+ basal and K10+ suprabasal epidermal layers. Scale bar = 50 μm. (H) Quantitation of

basement membrane length divided by tissue length in indicated genotypes. (I) Quantitation of proliferation, as assayed by BrdU incorporation, in control and KRASG12D mice. (J) Image showing co-localization of keratin 10 (red) and histone H2B (green) in a basal cell from a K10-rtTA; TRE-H2B-GFP mouse. (K) Quantitation of Keratin 10 positive basal cells in paw and backskin with indicated genotypes. (L) Fluorescence intensity (normalized) of β4-integrin in control and KRASG12D expressing footpad epidermis.

Supplementary Figures

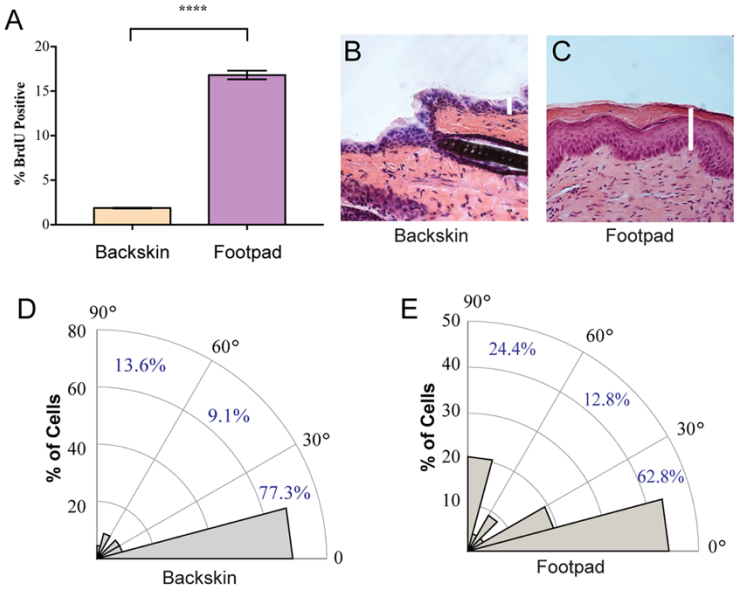

Supplementary Figure 1. Proliferation and spindle orientation differences between back and footpad skin. (A) Proliferation in WT backskin and footpad as measured by BrdU incorporation. (B,C) H&E images of WT backskin and footpad epidermis, showing their difference in thickness. (D,E) Radial histograms of mitotic spindles in WT backskin (n = 22) and footpad (n = 78) epidermis. Note that the data in Supplementary Figure 1D is the same as the data presented in Figure 2A.

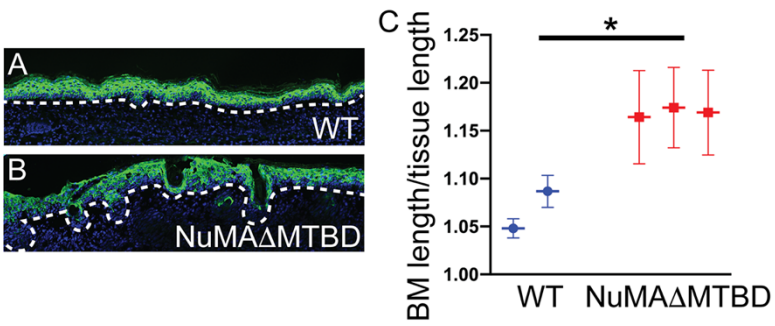

Supplementary Figure 2. Effect of TPA treatment on control and NuMA$^{\Delta MTBD}$ ear skin. Images show K10 (green) stained ear skin epidermis with the basement membrane noted with a dotted line. These mice were topically treated with TPA for ten days (treatment every second day). The graph indicates the basement membrane length/tissue length of the skin.